J Arid Land (2024) 16(1): 71–90
https://doi.org/10.1007/s40333-024-0001-7

Science Press Springer-Verlag

Land use change and its driving factors in the ecological function area: A case study in the Hedong Region of the Gansu Province, China

WEI Zhudeng*, DU Na, YU Wenzheng

School of Geographical Science, Nanjing University of Information Science & Technology, Nanjing 210044, China

Abstract: Land use and cover change (LUCC) is important for the provision of ecosystem services. An increasing number of recent studies link LUCC processes to ecosystem services and human well-being at different scales recently. However, the dynamic of land use and its drivers receive insufficient attention within ecological function areas, particularly in quantifying the dynamic roles of climate change and human activities on land use based on a long time series. This study utilizes geospatial analysis and geographical detectors to examine the temporal dynamics of land use patterns and their underlying drivers in the Hedong Region of the Gansu Province from 1990 to 2020. Results indicated that grassland, cropland, and forestland collectively accounted for approximately 99% of the total land area. Cropland initially increased and then decreased after 2000, while grassland decreased with fluctuations. In contrast, forestland and construction land were continuously expanded, with net growth areas of 6235.2 and 455.9 km^2, respectively. From 1990 to 2020, cropland was converted to grassland, and both of them were converted to forestland as a whole. The expansion of construction land primarily originated from cropland. From 2000 to 2005, land use experienced intensified temporal dynamics and a shift of relatively active zones from the central to the southeastern region. Grain yield, economic factors, and precipitation were the major factors accounting for most land use changes. Climatic impacts on land use changes were stronger before 1995, succeeded by the impact of animal husbandry during 1995–2000, followed by the impacts of grain production and gross domestic product (GDP) after 2000. Moreover, agricultural and pastoral activities, coupled with climate change, exhibited stronger enhancement effects after 2000 through their interaction with population and economic factors. These patterns closely correlated with ecological restoration projects in China since 1999. This study implies the importance of synergy between human activity and climate change for optimizing land use via ecological patterns in the ecological function area.

Keywords: land use; land type; geographic detector; driving mechanism; Hedong Region

Citation: WEI Zhudeng, DU Na, YU Wenzheng. 2024. Land use change and its driving factors in the ecological function area: A case study in the Hedong Region of the Gansu Province, China. Journal of Arid Land, 16(1): 71–90. https://doi.org/10.1007/s40333-024-0001-7

1 Introduction

Land use and cover change (LUCC) alters the Earth's energy balance and biogeochemical cycles, influencing land surface properties and ecosystem services (Foley et al., 2005; Turner et al., 2007; Lunyolo et al., 2021; Yan and Li, 2023). It is estimated that three-quarters of the Earth's land

*Corresponding author: WEI Zhudeng (E-mail: weizhudeng@126.com)
Received 2023-06-16; revised 2023-11-29; accepted 2023-12-26

surface has undergone human-induced alterations in the last millennium (Luyssaert et al., 2014). Within just six decades (1960–2019), almost a third of the global land area has experienced land use change, indicating a significant and accelerating transformation of land systems (Winkler et al., 2021). These substantial and escalating changes in land systems have led to a range of regional and global environmental challenges by influencing Earth's system processes. These challenges include impacts on carbon sources and sinks (Le Quéré et al., 2016), land degradation (Lambin and Meyfroidt, 2011), ecological productivity (Alkama et al., 2016; Li et al., 2019), climate change (Sy and Quesada, 2020), loss of habitat and species diversity (Powers and Jetz, 2019), decline of ecosystem services (Fang et al., 2022), and threats to food security (Turner et al., 2007). Consequently, LUCC has become a fundamental focus in prominent international scientific research programs such as the International Geosphere–Biosphere Programme (IGBP), International Human Dimensions Programme (IHDP) on Global Environmental Change, and Future Earth (Lambin et al., 1995; Turner et al., 1995; Future Earth, 2013).

Understanding the driving mechanisms and spatiotemporal patterns of LUCC is crucial for assessing the direction and extent of changes in land use and cover. This knowledge is essential for sustainable land use, enhancing ecosystem services, and mitigating global environmental challenges associated with LUCC (Li et al., 2020). Particularly, as the global population's consumption rate grows, heightened demand for natural resources and food will intensify stress on ecosystems, posing increasingly severe sustainability challenges for humanity.

In recent decades, a growing number of studies have focused on LUCC across various spatiotemporal scales. The key areas of interest encompass the detection of spatiotemporal LUCC processes, analysis of driving factors and mechanisms, construction of quantitative indicators, and simulation of LUCC processes (Halmy et al., 2015; Feng et al., 2021; Qacami et al., 2023). These studies aim to evaluate the ecological and social effects of LUCC at different scales. Under the influence of the Future Earth project, recent LUCC research has progressively shifted toward global sustainability. This evolution involves a focus on the coupling relationships among LUCC processes at different scales, ecosystem services, and human well-being (Dong et al., 2009; He et al., 2022; De Hertog et al., 2023; Refati et al., 2023).

Even though LUCC is a core issue, the driving mechanisms of land use change remain unclear. For instance, although there has been significant progress in quantifying the dynamics of land use change (Yang and Huang, 2021; Winkler et al., 2021), debates persist in monitoring land use dynamics. Song et al. (2018) reported a 7.1% increase in tree cover, challenging the prevailing view that global forest area has declined. Quantifying the relative contributions of various driving factors is particularly challenging. While anthropogenic activities are widely acknowledged as the direct and dominant drivers of LUCC at various spatial scales (Song et al., 2018; Damtea et al., 2020; Geng et al., 2023), other studies indicated an outweighed effect of natural factors compared with human factors (Batllori et al., 2020; Li et al., 2020), especially in ecologically fragile areas. Batllori et al. (2020) revealed that warming and drying climate led to a 10% conversion of forest land into shrub land and grassland. Climate change is considered the main reason for grassland degradation in Central Asia (Zhang et al., 2018). This complexity arises from the interaction of multiple factors influencing LUCC process. Land use intensity varies within a single land type, and transformations among different land types are intricate, as indicated by some studies (Erb et al., 2013; Parihar et al., 2018). Accordingly, strong geographically diverging characteristics of land use change process play a significant role (Winkler et al., 2021).

The Hedong Region in the Gansu Province serves as a typical area for investigating regional land use change processes and their underlying driving mechanisms, with a focus on ecological function maintenance and space optimization. Surrounded by the Qinghai-Tibet Plateau Eco-zone, the Sichuan-Yunnan and Loess Plateau Ecological Barrier, and the North Sand Prevention Belt (Wang et al., 2019; Long et al., 2023), the region is a crucial part of national ecological function areas in China (Fan, 2015). The Hedong Region's distinctive geographical characteristics raise the

following important questions: What are the characteristics of changes in local land use patterns over the past 30 years? How can we quantify the relative contribution of climate and human activities to land use dynamics? And what differences exist in the driving mechanisms of various factors on land use patterns over time or under different stages of ecological restoration projects? The present study utilizes an annual high-resolution LUCC dataset from 1990 to 2020 to analyze the spatiotemporal dynamics of land use in the Hedong Region. The primary objective of this study is to optimize ecological patterns, enhance land resource allocation, and promote sustainable development within designated ecological function areas.

2 Materials and methods

2.1 Study area

The Hedong Region (32°52′–37°30′N, 100°73′–108°73′E) is located in the east of the Yellow River in the Gansu Province, China. It is bordered by the Qinghai-Tibet Plateau to the west, the Qinling Mountains to the south, the Tengger Desert to the north, and the Loess Plateau to the east. The terrain slopes from west to east, showing a significant elevation variation ranging from 600 to 4830 m. The Gannan Plateau is characterized by a high-altitude cold and humid climate, while the other regions are influenced by the tailing edge of summer monsoon, resulting in a semi-arid and semi-humid climate. Consequently, the local ecosystem exhibits distinctive characteristics, serving as ecotones between forest, steppe, and agricultural land. In terms of land use, it represents a typical agro-pastoral transitional zone. Corresponding to the complex and diverse landforms, the ecological functions in the Hedong Region span a range from water conservation in the southwest to soil-water conservation in the northeast, sand fixation in the north, biodiversity protection in the south, and agricultural product provision in the central part. The administrative divisions include 9 prefecture-level cities (Lanzhou, Baiyin, Tianshui, Pingliang, Dingxi, Qingyang, Longnan, Linxia Hui Autonomous Prefecture, and Gannan Tibetan Autonomous Prefecture) and 67 counties, comprising a total area of 178×10^3 km^2.

2.2 Data sources and processing

Annual LUCC data from 1990 to 2020 were obtained from the Chinese Land Cover Yearly Data (CLCD) published by Yang and Huang (2021). The data have a high resolution of 30 m. The overall accuracy averaged 79.31% for nine land types. This dataset is widely used in recent studies on LUCC (Wang et al., 2022; Shao et al., 2024). In the present study, forest and shrub land were classified as "forest", while snow/ice, water, and wetland were classified as "water". Then, six major land use types used in the study were cropland, forest land, grassland, water body, bare land, and construction land.

Annual precipitation and annual average temperature data were derived from meteorological observations of 62 stations within the study area. The data source is from the National Meteorological Science Data Center of China (https://data.cma.cn/). County-level climatic data in the study area were obtained by averaging the values from meteorological stations within each county or through spatial interpolation.

Socio-economic statistical data at the county level were compiled from the Gansu Provincial Bureau of Statistics (https://tjj.gansu.gov.cn/), Gansu Economic Information Network (https://www.gsei.com.cn/), and the statistical yearbooks of various cities (prefectures) from 1990 to 2020. Seven indicators were selected, considering the land use characteristics and the advanced state of agriculture and animal husbandry in the Hedong Region (Table 1).

2.3 Methods

2.3.1 Land use transition matrix

Land use transition matrix is a widely used method to quantify area transformation in relation to different land use types between two periods. It helps understand the destination of each land type

Table 1 Data type and source of the study area

Data type	Index	Code	Unit	Source
Socioeconomic factor	Resident population	$X1$	Person	Gansu Provincial Bureau of Statistics, Gansu Economic Information Network, and the statistical yearbooks of cities (prefectures) from 1990 to 2020
	Large livestock inventory	$X2$	Sheep	
	Total GDP	$X3$	CNY	
	Added value of the primary industry	$X4$	CNY	
	Added value of the secondary industry	$X5$	CNY	
	Added value of the tertiary industry	$X6$	CNY	
	Grain yield	$X7$	kg	
Natural factor	Annual precipitation	$X8$	mm	Meteorological stations observations from National Meteorological Science Data Center of China
	Average annual temperature	$X9$	°C	
Land use change	Change rates of land use area	Y	km^2/a	CLCD product published by Yang and Huang (2021)

Note: GDP, gross domestic product; CNY, Chinese Yuan; CLCD, Chinese Land Cover Yearly Data.

at the initial period and the sources and composition of land use types at the final period (Lyu et al., 2018). The equation is as follows:

$$S_{ij} = \begin{vmatrix} S_{11} & S_{12} & \cdots & S_{1n} \\ S_{21} & S_{22} & \cdots & S_{2n} \\ \cdots & \cdots & \cdots & \cdots \\ S_{n1} & S_{n2} & \cdots & S_{nn} \end{vmatrix}, \tag{1}$$

where S_{ij} is the land area of transition from land use type i to j (km^2); and n is the number of land use types (n=6).

This study computes a land use transition matrix every five years to facilitate a comprehensive examination of dynamic characteristics of land use. This approach also enables the exploration of land use changes corresponding to different stages of ecological restoration projects. Furthermore, a transition matrix is specifically calculated from 1990 to 2020, providing an overview of the changes in land use during the past 30 a.

2.3.2 Land use dynamic degree

Land use dynamic degree index can reveal the quantity characters of certain land use change and represents the change rate of LUCC (Li et al., 2020). Dynamic degree for single land use type is calculated using Equation 2:

$$D = \frac{S_j - S_i}{S_i} \times \frac{1}{T} \times 100\%, \tag{2}$$

where D is the dynamic degree; S_i and S_j are the areas of land use type i in the initial and final years, respectively (km^2), and T is the time span between the initial and final years (a).

Dynamic degree of all land types is also known as comprehensive dynamic degree (the total changed area divided by the total area for all land types and time). This index is calculated to reflect the overall speed of land use change in the study area and to study regional differences in land use dynamics.

2.3.3 Geographical detector

Geographical detector is a new spatial statistical method that can be used to detect spatial heterogeneity and quantify the relative significance of driving forces on the dependent variable (Cao et al., 2013; Wang and Xu, 2017). The core idea of this method is that if a certain explanatory variable has an impact on the response variable, it will exhibit similar spatial distribution characteristics. Additionally, compared with other methods such as logistic regression model, this method has the advantage of immunity to multicollinearity among multiple explanatory variables (Wang and Xu, 2017). Geographical detector includes factor detectors, risk detectors, ecological detectors, and interactive detectors. Specifically, the factor detectors can

determine whether the explanatory variable X is the influencing factor of response variable Y (change rate of land use area) and explain the spatial differentiation mechanism of the response variable. It is represented by the q value as the following equation:

$$q = 1 - \frac{\sum_{h=1}^{L} N_h \sigma_h^2}{N\sigma^2}, \tag{3}$$

where L is the stratification of the response variable Y or explanatory factor X. In this study, it represents different-level rates of land area change at the county scale within the study area. N_h and N are the number of units in stratum h and the whole area, respectively; σ_h^2 and σ^2 are the variances of response variable Y values in stratum h and the whole area, respectively. The significance level is denoted by P value. A smaller P value and a q-statistic closer to 1 indicate a stronger explanatory power of the driving factor for land use change.

Besides, interactive detectors can evaluate whether the driving factors X_1 and X_2 have an interactive influence on a response variable Y. Interaction relationships can be determined by comparing the combined contribution (q value) of two individual factors and their independent contributions. In this study, we define both the nine explanatory variables ($X1$–$X9$; Table 1) and the response variable (Y; Table 1) at the county scale (67 counties in total) as the temporal change rates over study period. The rate of change is determined through simple linear regression. Additionally, it's important to note that data discretization can significantly impact detection results. In this study, the method provided by Cao et al. (2013) is employed to determine the optimal number of intervals and the discretization method. The result is listed in Table S1.

3 Results

3.1 Spatiotemporal pattern of LUCC

The spatial pattern of LUCC in the Hedong Region over the past 30 a is shown in Figure 1. It is evident that grassland, forest land, and cropland are the dominant land use types, constituting 99.00% of the total area. From the southeast to the northwest, a discernible distribution pattern emerges, transitioning from forest land to cropland and grassland. This phenomenon can be attributed to the diminishing hydrothermal conditions from southeast to northwest, influenced by the regional terrain and the circulation patterns of summer monsoon.

Grassland is the largest land use type, mainly distributed in the Gannan Plateau, as well as the northern parts of Lanzhou, Baiyin, and Qingyang cities. In 2020, the grassland area was 96,768.41 km^2, accounting for 54.42% of the total area. The cropland and forest land areas in 2020 were approximately equal with proportions of 23.02% and 21.38%, respectively. Cropland was predominantly concentrated in the central and eastern parts of the study area, with the majority situated in the Loess Plateau in eastern Gansu and the valley plain of the river system in the Longnan Mountains. In contrast, forest land is mainly distributed in the southern part, specifically within the Longnan Mountains (Fig. 1). Water body, construction land, and bare land had very small areas. In 2020, their proportions were 0.26%, 0.44%, and 0.48%, respectively. Construction land exhibited a distinct strip-shaped distribution, with major cities situated on both banks of rivers. This pattern reflects the constraining impact of water resources on human activities. Notably, Lanzhou City is located along the Yellow River, Tianshui City along the Weihe River, and Pingliang City along the Jinghe River. The primary urban area of the Lanzhou City made the largest contribution to the construction land. Water body mainly include rivers, reservoirs, wetlands, and snow/ice. The water bodies are the Liujiaxia Reservoir and the Yellow River in the Gansu Province. Wetlands and snow/ice were mainly distributed in the Maqu and Luqu counties in Gannan Tibetan Autonomous Prefecture. The bare land was mainly limited in the northern part.

A visual comparison of spatial distribution of land use across different time periods revealed a

discernible trend of expansion for forest land and construction land. The most notable expansion of construction land is observed around the cities of Lanzhou, Pingliang, and Tianshui. In the southeastern part (Fig. 1), forest land presented a visibly greener and more continuous pattern. Water body had relatively stable distribution.

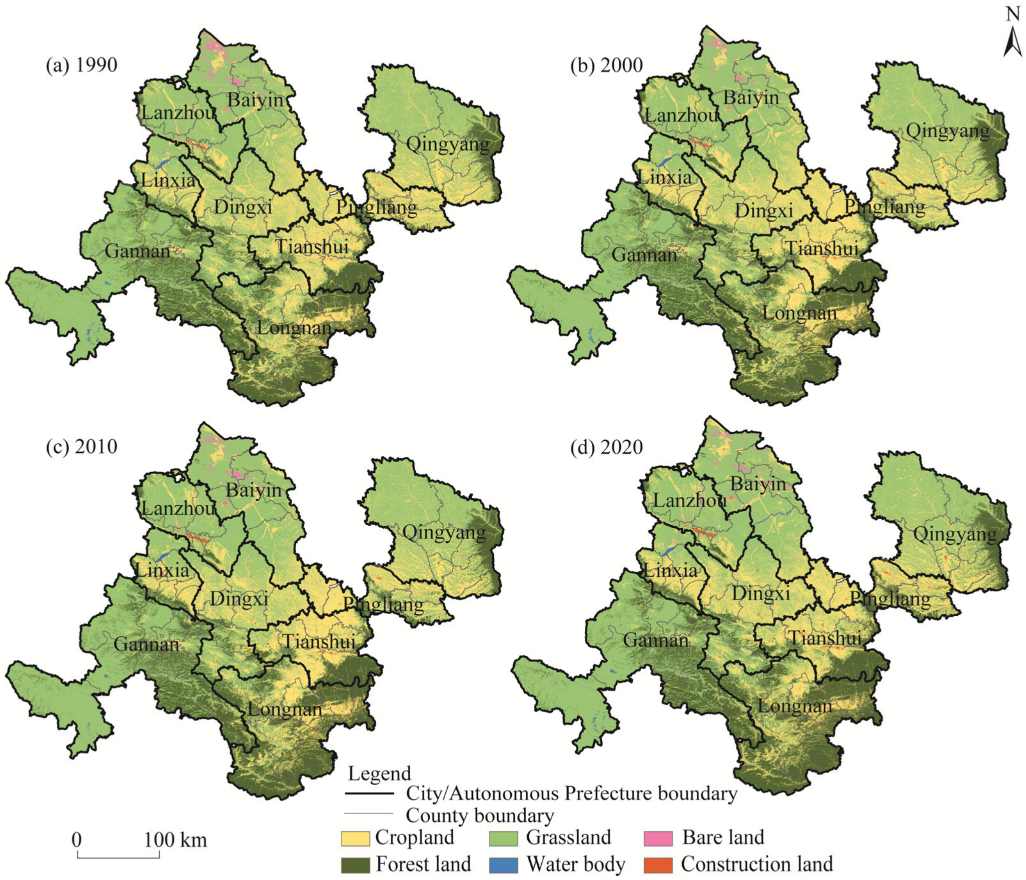

Fig. 1 Spatial distribution of land use in the Hedong Region from 1990 to 2020. (a), 1990; (b), 2000; (c), 2010; (d), 2020.

Table 2 provides statistics on the land use area in different years. It can be seen that grassland area had decreased and fluctuated from 1990 to 2020. The most significant change occurred from 1990 to 2000, with a net decrease of 4434.60 km^2. Cropland area showed an initial increase followed by a decrease trend. From 1990 to 2000, there was a net increase of 3114.11 km^2, while from 2000 to 2020, there was a net decrease of 5311.22 km^2. Forest land area exhibited a steady increase trend and had a net increase of 6235.24 km^2. Water body area had a small base and showed a decreasing trend followed by gradual recovery after 2010 to the initial level of 1990. Bare land area decreased sharply by half from 1990 to 2000 and gradually increased since 2000, showing significant fluctuations. Expansion of construction land was evident, with the area in 2020 exceeding twice that of 1990.

3.2 Characteristics and dynamics of land use conversion

3.2.1 Characteristics of land use conversion

Over the past 30 a, the study area has exhibited significant spatial variations in land use conversion (Fig. 2). Between 1990 and 2020, the converted land area totaled 31,430.90 km^2, with the primary conversions observed in grassland and cropland. Among other land use types, 12,251.06 km^2 of land was converted to grassland, of which 11,019.61 km^2 was converted from cropland, accounting for 90.00% of the total conversion area (Table 3). Additionally, 10,942.02

Table 2 Land use area and percentage in the Hedong Region from 1990 to 2020

Land type	1990		2000		2010		2020	
	Area (km^2)	Percentage (%)	Area (km^2)	Percentage (%)	Area (km^2)	Percentage (%)	Area (km^2)	Percentage (%)
Cropland	43,122.25	24.25	46,236.36	26.00	42,592.18	23.95	40,925.14	23.02
Forest land	31,790.77	17.88	33,567.97	18.88	35,077.61	19.73	38,026.00	21.38
Grassland	101,084.90	56.85	96,650.30	54.35	98,497.77	55.39	96,768.41	54.42
Water body	429.13	0.24	366.39	0.21	372.95	0.21	468.11	0.26
Construction land	325.93	0.18	432.48	0.24	600.95	0.34	781.83	0.44
Bare land	1064.33	0.60	563.77	0.32	675.81	0.38	847.78	0.48

km^2 of other lands was converted to cropland, with 96.00% of it coming from grassland. The conversion of forest land and barren land followed, with inflow areas of 556.09 and 592.11 km^2, respectively. However, both grassland and cropland areas decreased from 1990 to 2020 (Table 1). In contrast, the forest land area experienced a net increase of 6235.24 km^2. This indicated that there was a conversion of cropland into grassland, and both cropland and grassland underwent a transition to forest land as a whole from 1990 to 2020.

Grassland played a prominent role in the spatial distribution of land use conversions, covering most areas of the Hedong Region (Fig. 2). The expansion of cropland was predominantly observed in the Loess Plateau in eastern Gansu Province and the Longnan Mountains. The conversion of other lands to forest land occurred mainly in the Longnan Mountains, resulting primarily from the reduction of grassland. Therefore, mutual conversions among cropland, forestland, and grasslands mainly occurred at the connecting belts of the three land types. It was especially noticeable in the Longnan City, Tianshui City, and Qingyang City. The expansion of construction land was mainly concentrated in big cities at the expense of cropland. The conversion of other land use types to barren land mainly occurred in the northern parts of the Lanzhou and Baiyin cities. The increase in water body was mainly attributed to changes in wetland and snow/ice areas in the Gannan Tibetan Autonomous Prefecture, totaling 155.29 km^2 of land converted to water body. In addition, the construction of the Yingwu Reservoir in the Jingtai County in 2010, designed to support agricultural production and domestic water use in the northern part of the Baiyin City, contributed substantially to the expansion of water body in the northern part.

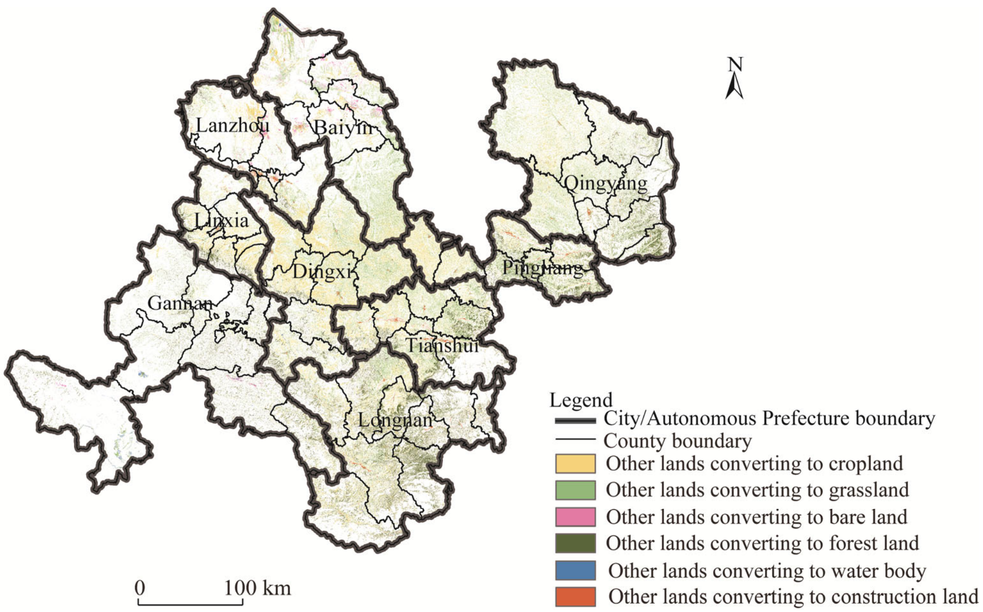

Fig. 2 Spatial distribution of conversion of land use in the Hedong Region from 1990 to 2020

Table 3 Land use transition matrix in the Hedong Region from 1990 to 2020

Land type	Cropland	Forest land	Grassland	Water body	Bare land	Construction land	Shrinkage
	(km^2)						
Cropland	29,983.12	1726.70	11,019.61	27.64	32.66	332.53	13,139.13
Forest land	330.91	30,902.50	556.09	0.73	0.00	0.53	888.26
Grassland	10,508.27	5391.43	84,517.35	105.98	462.47	99.37	16,567.52
Water body	13.44	5.28	83.04	312.82	1.83	12.71	116.30
Bare land	88.59	0.08	592.11	15.87	350.78	16.90	713.55
Construction land	0.82	0.00	0.21	5.07	0.04	319.79	6.14
Expansion	10,942.02	7123.50	12,251.06	155.29	496.99	462.04	-

Note: - means no value.

The extent of land use conversion varied across periods, with particularly pronounced changes between grassland and cropland due to their substantial proportions (Fig. 3). The most significant conversion from grassland to cropland occurred from 1990 to 1995, with an area of 7287.36 km^2. It was followed by the period during 2015–2020. From 2005 to 2010, the conversion to cropland was the lowest, with an area of 4043.45 km^2. In comparison, the most significant conversion from cropland to grassland occurred from 2010 to 2015, with an area of 6850.33 km^2. It was followed by the period during 2000–2005, with an area of 6568.73 km^2. The conversion of cropland to grassland decreased significantly from 2015 to 2020, with an area of 4885.45 km^2, which is the lowest level among the six periods. Regarding forest land, the area converted from other lands was consistently high for different periods. Almost all the net increased area was contributed from grassland and cropland, accounting for nearly 66.67% and 33.33%, respectively.

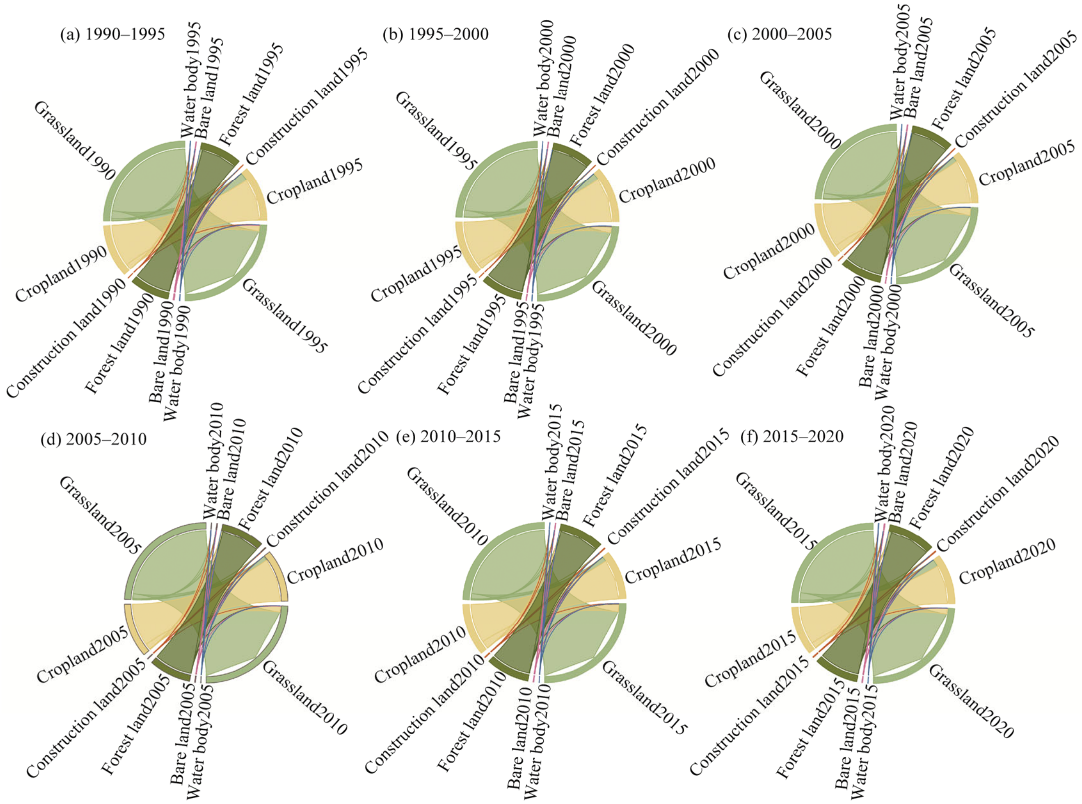

Fig. 3 Sankey diagram for five-year period changes in land use types in the Hedong Region from 1990 to 2020. Grassland1990 means the grassland area in 1990. (a), 1990–1995; (b), 1995–2000; (c), 2000–2005; (d), 2005–2010; (e), 2010–2015; (f), 2015–2020.

Additionally, due to such small base areas for water body, barren land, and construction land, land area transition for these three land types was minimal over a five-year period. Notably, barren land consistently contributed over 100.00 km^2 of its area as a supplement to grassland in each period. From 1990 to 1995, 505.79 km^2 of barren land was converted to grassland. The increase in construction land came from the transfer and supplementation of cropland and grassland in each period. The contribution of cropland reduction to construction land had exhibited an accelerated growth trend during four periods before 2010. The cropland reached its peak from 2005 to 2010, accounting for 60.00% of all other lands converted to construction land. While the remaining 40.00% is contributed by grassland.

3.2.2 Dynamics of land use conversion

The dynamic degree index reveals variations in both rate and direction of area change for each land use type across different periods (Fig. 4). It should be noted that construction land consistently exhibited a high and positive value in all six periods, indicating a continuous expansion trend in the Hedong Region over the past 30 a. Particularly, the dynamic degree reached 4.07% from 2005 to 2010. Bare land exhibited the most significant fluctuations among all land use types. Specifically, bare land decreased significantly from 1990 to 1995, with the largest dynamic degree of –8.87% among all land use types during all periods. In contrast, it showed a dramatic rebound from 2000 to 2005 and from 2015 to 2020, with expansion exceeding that of construction land. The dynamic change of water body experienced a significant reduction from 1995 to 2000 and a significant expansion from 2015 to 2020. Cropland, forest land, and grassland underwent relatively narrow fluctuations of decrease or expansion in dynamic changes throughout all periods.

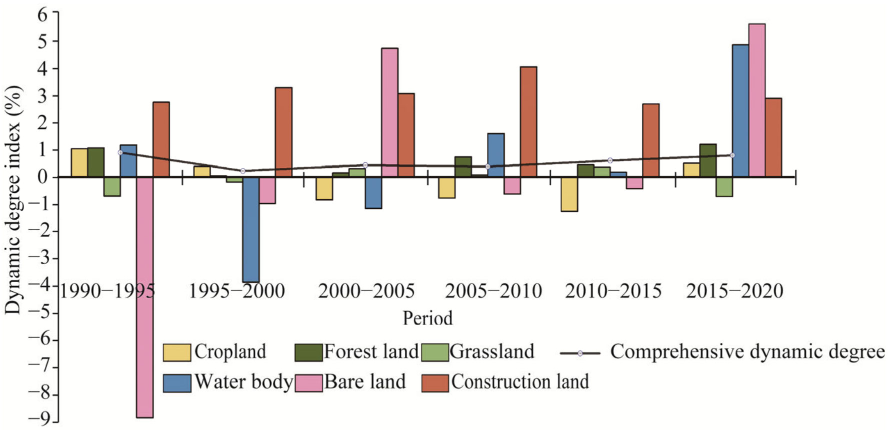

Fig. 4 Dynamic degree index of land use types in the Hedong Region from 1990 to 2020

Dynamic degree of land use can reflect the overall land use change influenced by various factors. The results show a dynamic degree of 0.25% from 1990 to 2020. The average dynamic degree across all periods for the study area during the same time scale is 0.56%, more than twice the initial value. This suggests that the degree of natural and human activities' impact on land use had significant temporal differentiation. Exploring land use change characteristics in different periods can provide more detailed insights into the impacts of driving factors on land use changes. From Figure 4, the most active dynamic changes in land occurred from 1990 to 1995 and from 2015 to 2020, with the rates of 0.90% and 0.80%, respectively. The period from 2010 to 2015 ranked second, with a rate of 0.60%. Since 2000, the comprehensive dynamic degree of land use in the entire region has increased on average by 0.15% on the basis of 0.23% during 1995–2000 in each five-year period. It reached 0.80% during 2015–2020, indicating the steadily rising impact of driving forces on land use.

Moreover, significant spatial variations in the dynamics of county-level land use occurred

across different periods. As shown in Figure 5, the dynamic changes in land use primarily occurred in the central and eastern parts of the study area. In general, the most significant change occurred from 1990 to 1995, with Jingning County in the Pingliang City experiencing the highest comprehensive dynamic degree (6.96%) of land use. From 2005 to 2010, the overall change was relatively moderate, with Chongxin County in the Pingliang City having the highest comprehensive dynamic degree (3.69%) of land use. The counties with strong dynamic changes of land use changed through time. However, the clustering areas with higher dynamic rate showed an overall shifting trend from the central part to the east and southeast (Fig. 5). The dynamic changes in the northern counties gradually shifted from active to inactive. The comprehensive dynamic changes in the northern parts of the study area, mainly in the Lanzhou and Baiyin cities, gradually stabilized after 2005. In contrast, the southeastern counties became more active in land use after 2005. The spatiotemporal fluctuations of land use in the Longnan City were very obvious. Also, some counties exhibited stable changes of land use, such as the Maqu County in the Gannan Tibetan Autonomous Prefecture. It maintained the lowest level of dynamic changes, possibly due to its plateau environment and low population density.

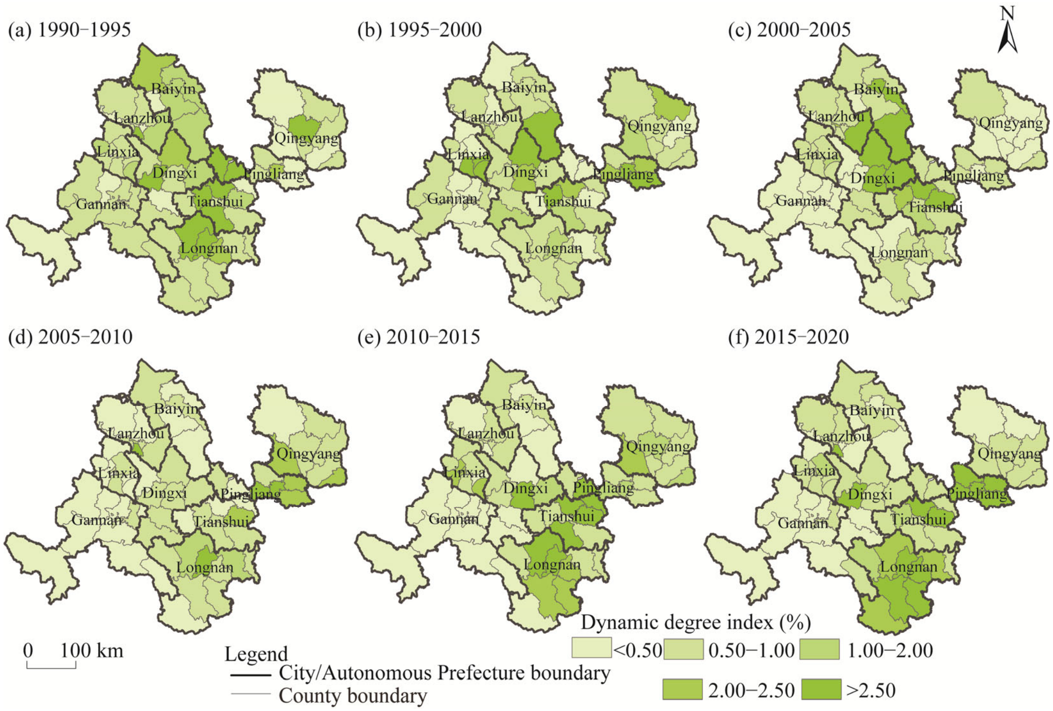

Fig. 5 Spatial distribution of county-level land use dynamics for different periods from 1990 to 2020. (a), 1990–1995; (b), 1995–2000; (c), 2000–2005; (d), 2005–2010; (e), 2010–2015; (f), 2015–2020.

3.3 Driving factors of LUCC and dynamics

3.3.1 Driving factors of LUCC

A low explanatory power of each factor for the change rates of six land use types over the past 30 a is shown in Table 4. The order of factors affecting land use changes in cropland was grain yield (0.42)>GDP (0.36)>secondary industry (0.35)=precipitation (0.35)>primary industry (0.23). The Hedong Region still relies on agricultural production as its basic economic source. However, the local population decreased in past decades. The region faces multiple challenges, including the strain on agricultural economic inputs, adverse natural conditions, and food security, resulting in fluctuations in arable land area in the Hedong Region. The main driving factor for forest land is GDP, with a q value of 0.45, followed by secondary industry. This indicates that changes in forest land are mainly influenced by changes in human economic intervention. The order of factors in

grassland was grain yield (0.58)>precipitation (0.46)>GDP (0.40)>tertiary industry (0.25)>primary industry (0.20). Both grain yield and GDP have a close relationship with the effectiveness of ecological projects, such as returning farmland to forest land and grassland, while precipitation directly affects grass growth.

The primary driving factors for water body are GDP (0.49) and precipitation (0.48), followed by livestock inventory (0.32). Precipitation is vital for water supply in the Hedong Region, where water resource heavily relies on precipitation. In semi-arid areas, livestock requires a substantial water resources. The main factor influencing construction land is the level of socio-economic development, with the dominant factors being the added values of three industries and GDP.

Table 4 Explained variance of driving factors for land use change from 1990 to 2020

Code	Cropland	*P* value	Forest land	*P* value	Grassland	*P* value	Water body	*P* value	Bare land	*P* value	Construction land	*P* value
*X*1	0.24	0.20	0.20	0.28	0.15	0.37	0.11	0.63	0.10	0.70	0.11	0.59
*X*2	0.26	0.20	0.21	0.06	0.29	0.15	0.32	0.01	0.10	0.66	0.23	0.07
*X*3	0.36	0.01	0.45	0.00	0.40	0.00	0.49	0.00	0.14	0.15	0.35	0.01
*X*4	0.23	0.02	0.09	0.59	0.20	0.03	0.11	0.59	0.14	0.45	0.30	0.02
*X*5	0.35	0.00	0.26	0.04	0.24	0.10	0.09	0.73	0.13	0.48	0.36	0.00
*X*6	0.23	0.07	0.12	0.40	0.25	0.05	0.09	0.75	0.09	0.62	0.45	0.00
*X*7	0.42	0.00	0.19	0.21	0.58	0.00	0.11	0.47	0.14	0.43	0.20	0.12
*X*8	0.35	0.00	0.18	0.37	0.46	0.00	0.48	0.01	0.10	0.67	0.12	0.59
*X*9	0.12	0.44	0.23	0.10	0.10	0.66	0.15	0.29	0.19	0.22	0.18	0.24

Note: *X*1–*X*9 mean nine explanatory variables that are listed in Table 1.

Interactive detection further reflects the coupling effects of two factors on land use change (Fig. 6). And bifactor analysis is discernible for specific factors, particularly for cropland, forest land, grassland, and construction land. For cropland, the interactive effects followed a hierarchy of GDP∩population (0.74)=GDP∩secondary industry>GDP∩tertiary industry>secondary industry ∩temperature. This suggests that interactive effects involving GDP or secondary industry and other factors exhibited heightened explanatory power for cropland. Even when considering grain yield, the interactive effects for GDP∩grain yield and secondary industry ∩ grain yield demonstrated enhanced effect of bifactor. Changes in GDP or secondary industry, coupled with alterations in annual precipitation and temperature, were also observed to augment explanatory power. Similarly, the interaction effects of nine factors on forest land displayed more pronounced nonlinear enhanced effects, particularly for GDP, population, grain yield, precipitation, and temperature, which exhibited enhanced effects in their interaction with other factors. The most interactive effects followed a hierarchy of GDP∩secondary industry (0.80)>secondary industry∩temperature (0.65)>GDP∩grain yield (0.63). For grassland, the stronger interactive effects were observed in the order of GDP∩secondary industry (0.64)>GDP∩grain yield (0.63)>GDP∩large livestock inventory (0.62).

For construction land, the most notable interactive effects were found between grain yield, tertiary industry, secondary industry, and other factors. For water body, only the interaction effect for grain yield∩GDP showed a higher explanatory power of 0.68. For bare land, interactions between temperature or precipitation and other factors showed a stronger nonlinear effect, with the highest explanatory power reaching 0.59.

In summary, the primary driver factors for land use types were grain yield, GDP, and precipitation. For coupling effects, the dominant interactive factors are economic factors (GDP and secondary industry) and others, followed by the interaction between grain yield and other factors. For cropland, the impact of temperature on cropland was more pronounced than precipitation. Conversely, temperature and precipitation equally enhanced changes in forest land

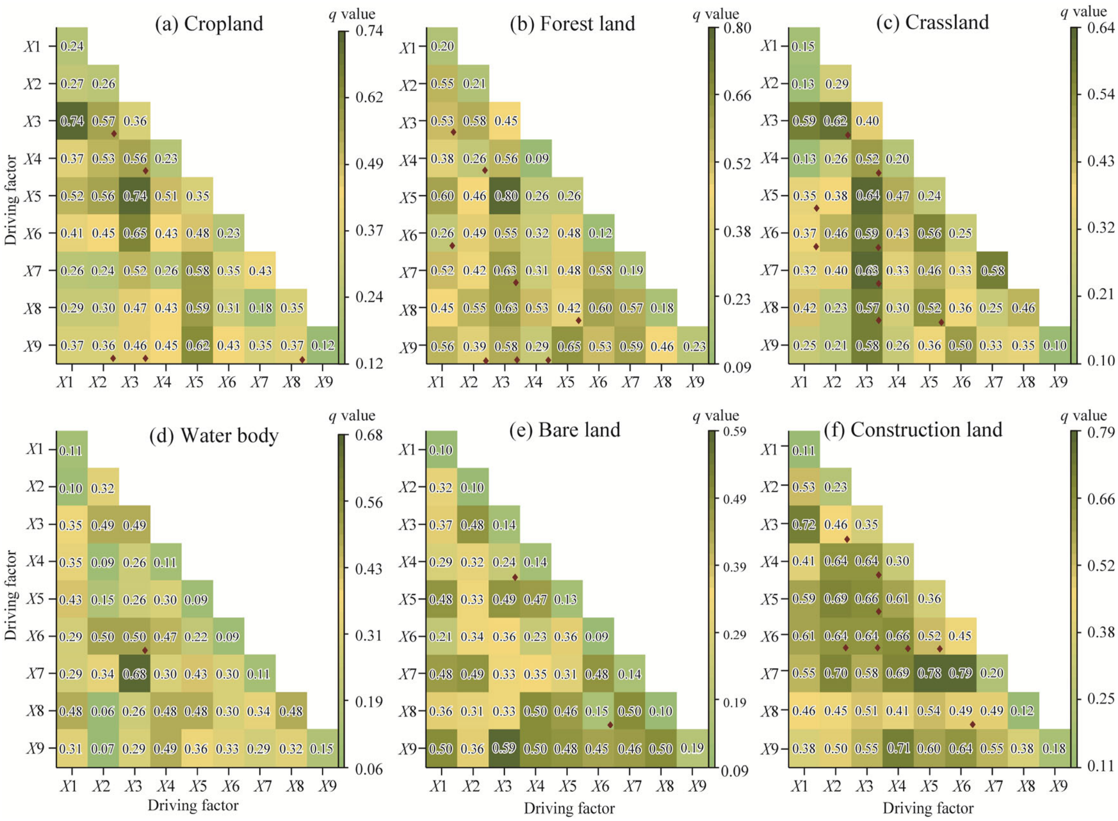

Fig. 6 Interactive effects of driving factors for land use change from 1990 to 2020. The red dots indicate enhanced effect of bifactor. (a), cropland; (b), forest land; (c), grassland; (d), water body; (e), bare land; (f), construction land. *X*1–*X*9 mean nine explanatory variables that are listed in Table 1.

and grassland when interacting with other factors. Moreover, the influence of a large livestock inventory on grassland experienced significant enhancement through interaction with GDP. Construction land showed sensitivity to various factor interactions, particularly those involving grain yield and industries.

3.3.2 Dynamics

For different periods, the dominant drivers for the six land types varied. The dominant factors for different land types also differed in the same period. As shown in Figure 7, the dominant factors of grain yield had the strongest explanatory power in the periods of 2000–2005 (q value reached as high as 0.59), 2005–2010, and 2010–2015 for cropland. Besides, the impacts of precipitation and temperature on cropland and grassland both fluctuated with time, with the periods of 2005–2010, 2010–2015, and 1990–1995 having better explanatory power. The difference was that the livestock inventory had higher explanatory power in the periods of 1995–2000 and 2015–2020 for grassland. For forest land, GDP became particularly pronounced after the year 2000. Besides, livestock inventory had a relatively better contribution to forest land during 2005–2020 than those of other periods. Especially for 2015–2020, livestock inventory had the strongest explanatory power. Precipitation had the strongest explanatory power for the periods of 1990–1995, 2005–2010, and 2010–2015 (Fig. 7). In summary, the primary drivers for cropland successively shifted from temperature to livestock inventory and grain yield. Similarly, for grassland, the dominant drivers successively changed from temperature to livestock inventory, grain yield, precipitation. As for forest land, the dominant drivers successively transitioned from precipitation to population, GDP, precipitation, and livestock inventory. The results indicated the significant impacts of climate change before 1995 changed to the impact of animal husbandry during 1995–2000, and followed by the impacts of grain production and GDP after 2000 (2000–2015).

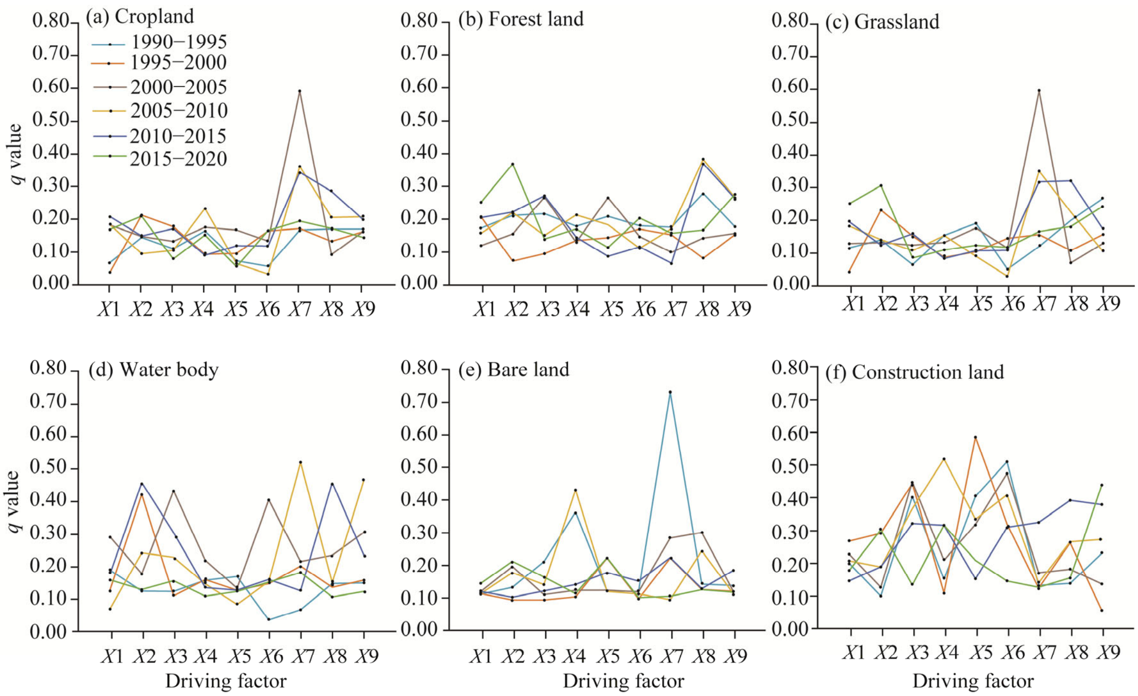

Fig. 7 Single-factor analysis for driving land use change from 1990 to 2020. (a), cropland; (b), forest land; (c), grassland; (d), water body; (e), bare land; (f), construction land. *X*1–*X*9 mean nine explanatory variables that are listed in Table 1.

The predominant driving factors in water body varied in different periods. The dominant drivers changed from population to livestock inventory, GDP, grain yield, precipitation, and grain yield. Grain yield emerged as the primary driving factor for bare land during 1990–2000 and 2010–2015, followed by precipitation or grain yield during 2000–2005, and the primary industry during 2005–2010. This signifies that grain production and precipitation played pivotal roles in driving changes in bare land across different periods. For construction land, the dominant factors underwent a shift from three industries combined with GDP to climate changes. This suggests a potential constraint imposed by climate change on the expansion of construction land.

Interaction detection analysis shows that the combined effects of different factors on land use changes also varied across different periods (Fig. 8). The interaction effects on cropland were strong after 2000. It was significant between population and secondary industry/temperature/grain yield/precipitation during 2000–2010, and between grain yield and precipitation/large livestock inventory/temperature during 2010–2020. The climatic impact became notably more pronounced due to interactions with other factors after 2000. For forest land, the interactive effects of factors exhibited an upward trend after 2005, especially during 2005–2010 and 2015–2020. Overall, the stronger interactions were identified between large livestock inventory and grain yield/secondary industry/population/temperature, between grain yield and population/secondary industry, and between population and precipitation (Fig. 8). For grassland, the interactive enhancement effects were relatively lower during 2000–2005 and reached their peak during 2015–2020, especially the interaction between grain yield and climate change. This suggests that grain yield and climate change could exert a stronger influence on grassland.

For water body, nonlinear enhancement significantly occurred during 2000–2005. The enhancement effect on bare land changes was generally more significant during 1990–1995 and 2005–2010. Interaction between grain produce or climatic change and other factors could more significantly impact the bare land. For construction land, the interaction effects culminated during 2000–2005.

In summary, interactive effects among various factors on different land uses displayed

considerable complexity over time. Broadly, agricultural activities (reflected in grain yield), pastoral endeavors (represented by livestock inventory), and climate change exhibited heightened enhancement after 2000 through their interactions with population and economic factors.

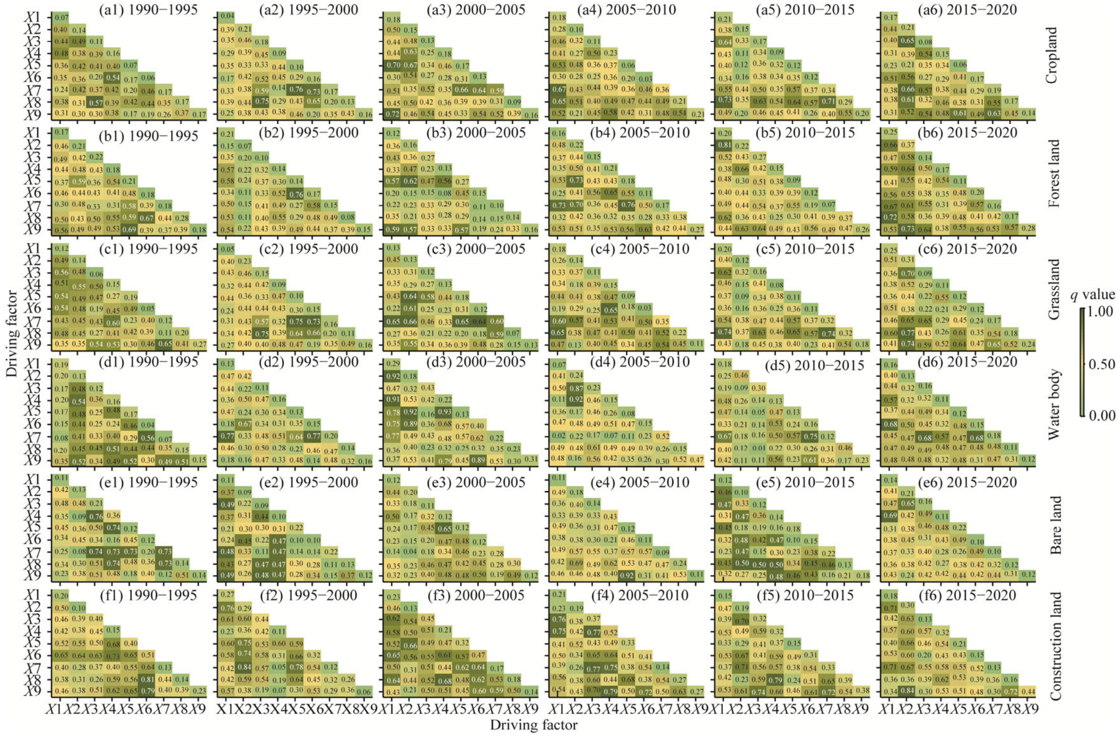

Fig. 8 Interaction detection of driving factors for land use change in different periods from 1990 to 2020. a–f are the changes of the cropland, forest land, grassland, water body, bare land, and construction land in different periods (1990–1995, 1995–2000, 2000–2005, 2005–2010, 2010–2015, and 2015–2020), respectively. $X1$–$X9$ mean nine explanatory variables that are listed in Table 1

4 Discussion

4.1 Driving mechanism of LUCC

Previous studies have identified LUCC and their associated factors in different regions, such as Northwest China (Yan et al., 2019b), the Taperoá River basin in northeastern Brazil (Silva et al., 2020), the north-western coastal desert of Egypt (Halmy et al., 2015), Jimma Geneti District in western Ethiopia (Hailu et al., 2020), and the Middle Suluh Valley in northern Ethiopia (Hishe et al., 2020). Many studies revealed LUCC pattern characterized by agricultural land expansion at the expense of woodland, grassland, and wetland over the past decades. For instance, Hailu et al. (2020) reported that in the Jimma Geneti District, wetlands declined by 19.2% from 1973 to 2019. Conversely, the most dominant cultivated land increased by 13.0% at a rate of 7.4 km²/a. This pattern appears similar to the land use dynamics in the Hedong Region before 2000. However, it is not applicable after 2000.

This study suggests a division of land use and cover in the Hedong Region into two primary stages during 2000–2005. The land use dynamics were significantly different between these two stages. In the first stage (1990–2000), the land use transition structure was not conducive to enhancing ecological function, environmental sustainability, and socioeconomic well-being. Construction land encroached on cultivated land, and, in a quest for more food, grasslands, bare land, and water body were reclaimed as cultivated land. These practices resulted in ecological problems, such as desertification and sandstorms (Li et al., 2004). Although local forests

increased during this stage, it was largely a result of the Three-North Forest Shelterbelts Program launched in 1979 in China (Bennett, 2008). However, some studies indicated that this increase in forest land was mainly achieved by destroying grassland and farmland, as only a small area of unused lands were converted in the Gansu Province (Li et al., 2020).

In the second stage (2000–2020), the land use structure in the Hedong Region tended to become more rational. This trend extended beyond the Hedong Region to encompass the broader scale of the entire Yellow River basin in China, particularly after 2005 (Deng et al., 2022; Song et al., 2022). This positive shift was primarily attributed to major ecological restoration programs, such as the Natural Forest Protection Program launched in 1998 (Xu et al., 2006) and the Grain for Green Project initiated in 1999 (Bennett, 2008; Song et al., 2022). These ecological projects have directly impacted local land use, recognized as key driving factors of LUCC (Deng et al., 2022; Song et al., 2022). Consequently, cropland and grassland gradually transformed into forest land, contributing to an overall increase in the dynamic degree of land use in the Hedong Region since 2000. Furthermore, the dominant factors influencing land use changes increasingly leaned towards grain production, GDP, and the added value of secondary industry, as interactive enhancement effects intensified after 2000, especially for the three major land use types: grassland, forest land, and cropland. The spatial shift in the land use activity center from the central to the southeastern parts around 2005 was also linked to ecological restoration programs. The Longnan Mountains was included in the Yangtze River Shelter-Forest Project Phase II (2001–2010) and III (2011–2020). Moreover, the second phase of the Grain for Green Project starting in 2014 focused more on sloping land conversion and gully reclamation (Deng et al., 2022). It aligned with the broader goals of building a moderately prosperous society, poverty alleviation, and ecological security construction (Jin et al., 2016). These efforts were instrumental in stimulating land use activities, particularly in the southeastern mountainous area of the Hedong Region, as evidenced by the changes in forest land (Fig. 2). This contrasts sharply with the impact of deforestation on land degradation in other regions, such as North Africa (Zerouali et al., 2023).

However, land uses in the Hedong Region over the past 30 retained strong regional characteristics. It diverges from the LUCC situation of the Gansu Province as a whole, where forest land, grassland, cropland, and water body significantly increased from 2005 to 2018 (Li et al., 2020). Urban expansion in the Gansu Province mainly occupied unused lands rather than lands with more ecological benefits, such as forest land and grassland, after 2005 (Li et al., 2020). In the Hedong Region from 2000 to 2020, the expansion of construction land primarily occurred at the expense of cropland. Cropland had a positive contribution to grassland, and both cropland and grassland positively contributed to forest land as a whole. However, the underlying driving mechanisms were likely different from those before 2000. This study identifies grain yield, GDP, and second industry as major factors influencing most land use changes after 2000. Their driving mechanisms were closely related to ecological restoration programs. Taking grain yield as an example, the grain yield in the study area showed an upward trend, which was mainly driven by counties with developed agriculture. However, this contradicted the declining trend in cropland after 2000. Thus, increasing grain production might not be the direct driving force for land use transition; instead, the driving mechanism conveyed by grain yield was related to ecological restoration programs. Of course, further verification of this mechanism is warranted. The significant increase in forest land, coupled with a controlled reduction in grassland, could mitigate the environmental impacts of construction land expansion after 2000. The extensive expansion of construction land in the study area might be associated with increasing population, primarily due to migration from rural areas to major cities (Jin et al., 2016), leading to an increase in abandoned arable land to some extent (Hu et al., 2014).

In comparison with precipitation and temperature, grain yield and economic factors demonstrated superior explanatory power for land use changes in the Hedong Region. Nevertheless, climatic impacts, especially on grasslands (Dong et al., 2009), should not be underestimated. Numerous studies have emphasized the importance of climate change in driving the grassland (Yuan et al., 2015). Some scholars suggested that climate of the Loess Plateau

tended to be warm and humid, conducive to the implementation of sloping land conversion program from 2000 to 2018 (Deng et al., 2022). Nevertheless, since the 1990s, there has been a noticeable increase in temperature but a decreasing trend in precipitation in the Hedong Region (Zhao et al., 2012). Li et al. (2020) highlighted that natural factors were the primary force influencing changes in LUCC in the Gansu Province from 1980 to 2018. The climatic impact could be amplified through interactions with socioeconomic factors such as overgrazing (Yan et al., 2019a).

Our findings align with studies emphasizing the role of environmental protection policies in contributing to vegetation recovery in Northwest China and Northern Africa (Hishe et al., 2020). The conclusion on driving factors is consistent with the study in Gannan Tibetan Autonomous Prefecture (Liu et al., 2014), but differs from the notion that natural factors were generally the main force influencing changes in LUCC in the Gansu Province, possibly due to the larger arid and semi-arid areas in the Gansu Province. Moreover, compared with previous studies, this study provides more detailed driving mechanisms for the evolution of land use spatial patterns in the ecological function areas. The climatic impacts on land use changes were stronger before 1995, succeeded by the impact of animal husbandry during 1995–2000, followed by the impacts of grain production and GDP after 2000. Given its unique position within ecological function areas in the Hedong Region of the Gansu Province, land use changes are shaped by the coupling effects of climate change, ecological construction, and socioeconomic development.

4.2 Limitations

This study primarily employed the geographical detectors method to analyze the driving factors of LUCC. While geographical detectors have the advantage of determining dominant factors influencing LUCC spatial patterns, it falls short in identifying direct and indirect factors, as well as driving pathways. Consequently, this study may not fully elucidate the intricate driving mechanisms of interactive factors. Other applicable methods, such as the random forest algorithm (Leroux et al., 2017), correlation network analysis (Kleyer et al., 2019), and structural equation modeling (Grace and Keeley, 2006), could be employed for comparison or to quantify interactions among drivers of land use changes in future research. Moreover, due to limitations in data acquisition, this study only considers indices of representative driving factors. For instance, the impact of ecological restoration projects on local LUCC is significant. The study did not use direct indicators of policy to quantify the influence of ecological programs, relying solely on economic indicators to measure the impact factors of construction land expansion. This might affect the analysis results regarding the influence of relevant policies on land use dynamics. Therefore, the selection of multidimensional indicators requires further consideration.

5 Conclusions

This study examined the temporal dynamics of land use patterns and their underlying drivers in the Hedong Region of the Gansu Province from 1990 to 2020. We found that grassland, cropland, and forest land accounted for approximately 99% of the total land area. From 1990 to 2020, the transition in land use indicated a shift from cropland to grassland, and both cropland and grassland underwent conversion to forest land. This pattern has contributed to the expansion of forest land. The continuous expansion of construction land primarily originated from cropland. During 2000–2005, land use experienced intensified temporal dynamics and a shift of relatively active zones from central to southeastern parts. Generally, grain yield and economic factors demonstrated superior explanatory power for land use changes, followed by precipitation. However, there was a relatively stronger impact of climate change before 1995, succeeded by the impact of animal husbandry during 1995–2000, followed by the impacts of grain yield and GDP after 2000. Agricultural and pastoral activities, coupled with climate change, exhibited heightened nonlinear or bifactor enhanced effect after 2000, influenced by their intricate interaction with population and economic factors. These patterns closely correlate with ecological restoration

projects in China since 1999.

This study highlights the importance of considering the interrelated effects of climate change, socioeconomic development, and ecological construction. Particularly, the study underscores the pronounced synergistic effects between human activities and climate change on land use since 2000 due to the Grain for Green Project in China. Therefore, a balanced approach is recommended to ensure the sustainability of land use and ecological system in these areas.

Conflict of interest

The authors declare that they have no known competing financial interests or personal relationships that could have appeared to influence the work reported in this paper.

Acknowledgements

This study was funded by the National Natural Science Foundation of China (U20A2098, 41701219) and the National Key Research and Development Program of China (2019YFC0507801). The authors appreciate the anonymous reviewers for their constructive comments and suggestions.

Author contributions

Conceptualization: WEI Zhudeng; Methodology: WEI Zhudeng, DU Na; Formal analysis: WEI Zhudeng, DU Na; Writing - original draft preparation: DU Na; Writing - review and editing: WEI Zhudeng, YU Wenzheng; Funding acquisition: WEI Zhudeng, YU Wenzheng; Resources: WEI Zhudeng, DU Na; Supervision: WEI Zhudeng. All authors approved the manuscript.

References

Alkama R, Cescatti A. 2016. Biophysical climate impacts of recent changes in global forest cover. Science, 351(6273): 600–604.

Batllori E, Lloret F, Aakala T, et al. 2020. Forest and woodland replacement patterns following drought-related mortality. Proceedings of the National Academy of Sciences of the United States of America, 117(47): 29720–29729.

Bennett M T. 2008. China's sloping land conversion program: Institutional innovation or business as usual? Ecological Economics, 65(4): 699–711.

Cao F, Ge Y, Wang J. 2013. Optimal discretization for geographical detectors-based risk assessment. GIScience & Remote Sensing, 50(1): 78–92.

Damtea W G, Kim D, Im S. 2020. Spatiotemporal analysis of land cover changes in the Chemoga Basin, Ethiopia, using Landsat and Google Earth images. Sustainability, 12(9): 3607, doi: 10.3390/su12093607.

De Hertog S J, Havermann F, Vanderkelen I, et al. 2023. The biogeophysical effects of idealized land cover and land management changes in Earth system models. Earth System Dynamics, 14(3): 629–667.

Deng Y, Jia L, Guo Y, et al. 2022. Evaluation of the ecological effects of ecological restoration programs: A case study of the sloping land conversion program on the Loess Plateau, China. International Journal of Environmental Research and Public Health, 19: 7841, doi: 10.3390/ijerph19137841.

Dong L, Wang W, Ma M, et al. 2009. The change of land cover and land use and its impact factors in upriver key regions of the Yellow River. International Journal of Remote Sensing, 30(5): 1251–1265.

Erb K H, Haberl H, Jepsen M R, et al. 2013. A conceptual framework for analysing and measuring land-use intensity. Current Opinion in Environmental Sustainability, 5(5): 464–470.

Fan J. 2015. Draft of major function oriented zoning of China. Acta Geographica Sinica, 70(2): 186–201. (in Chinese)

Fang Z, Ding T, Chen J, et al. 2022. Impacts of land use/land cover changes on ecosystem services in ecologically fragile regions. Science of the Total Environment, 831: 154967, doi: 10.1016/j.scitotenv.2022.154967.

Feng Y, Zhu J, Zeng L, et al. 2021. Profit and loss prediction of ecosystem service value under county land use change: A case study of Banan District, Chongqing. Acta Ecologica Sinica, 41(9): 3381–3393. (in Chinese)

Foley J A, DeFries R, Asner G P, et al. 2005. Global consequences of land use. Science, 309(5734): 570–574.

Future Earth. 2013. Future Earth Initial Design: Report of the Transition Team. Paris: International Council for Science (ICSU).

Geng X, Hu S, Wang X, et al. 2023. Adaptive change of land use to nature and society in China's agro-pastoral ecotone. Land Use Policy, 126: 106554, doi: 10.1016/j.landusepol.2023.106554.

Grace J B, Keeley J E. 2006. A structural equation model analysis of post fire plant diversity in California shrub lands. Ecological Applications, 16(2): 503–514.

Hailu A, Mammo S, Kidane M. 2020. Dynamics of land use, land cover change trend and its drivers in Jimma Geneti District, Western Ethiopia. Journal of Land Use Policy, 99: 105011, doi: 10.1016/j.landusepol.2020.105011.

Halmy M W A, Gessler P E, Hicke J A, et al. 2015. Land use/land cover change detection and prediction in the north-western coastal desert of Egypt using Markov-CA. Applied Geography, 63: 101–112.

He C, Zhang J, Liu Z, et al. 2022. Characteristics and progress of land use/cover change research during 1990–2018. Journal of Geographical Sciences, 32(3): 537–559. (in Chinese)

Hishe S, Bewket W, Nyssen J, et al. 2020. Analysing past land use land cover change and CA-Markov-based future modelling in the middle Suluh Valley, Northern Ethiopia. Geocarto International, 35(3): 225–255.

Hu Y, Hu S, Yao J. 2014. Factors affecting farmland abandonment behavior of farmers in semi-arid regions of Gansu Province. Guizhou Agricultural Sciences, 42(9): 227–231. (in Chinese)

Jin S, Li B, Yang Y, et al. 2016. Basic characteristics and pattern of land use change in Gansu Province. Journal of Lanzhou University: Natural Science, 52(3): 334–341. (in Chinese)

Kleyer M, Trinogga J, Cebrián-Piqueras M A, et al. 2019. Trait correlation network analysis identifies biomass allocation traits and stem specific length as hub traits in herbaceous perennial plants. Journal of Ecology, 107(2): 829–842.

Lambin E F, Baulies X, Bockstael N, et al. 1995. Land-use and land-cover change (LUCC): Implementation strategy. A core project of the International Geospere-Biosphere Programme and the International Human Dimensions Programme on Global Environmental Change. In: IGBP Report 48. IHDP Report 10. IGBP, Stockholm, Sweden.

Lambin E F, Meyfroidt P. 2011. Global land use change, economic globalization, and the looming land scarcity. Proceedings of the National Academy of Sciences of the United States of America, 108(9): 3465–3472.

Le Quéré C, Andrew R M, Canadell J G, et al. 2016. Global carbon budget 2016. Earth System Science Data, 8(2): 605–649.

Leroux L, Begue A, Lo Seen D, et al. 2017. Driving forces of recent vegetation changes in the Sahel: Lessons learned from regional and local level analyses. Remote Sensing of Environment, 191: 38–54.

Li G, Sun S B, Han J C, et al. 2019. Impacts of Chinese Grain for Green program and climate change on vegetation in the Loess Plateau during 1982–2015. Science of the Total Environment, 660: 177–187.

Li K, Feng M, Biswas A, et al. 2020. Driving factors and future prediction of land use and cover change based on satellite remote sensing data by the LCM model: A case study from Gansu Province, China. Sensors, 20(10): 2757, doi: 10.3390/s20102757.

Li X Y, Wang L X, Zhang Y S. 2004. Analysis of roles of human activities in land desertification in arid area of Northwest China. Scientia Geographica Sinica, 24(1): 68–75. (in Chinese)

Liu J, Kuang W, Zhang Z, et al. 2014. Spatiotemporal characteristics, patterns, and causes of land-use changes in China since the late 1980s. Journal of Geographical Sciences, 24: 195–210.

Long Y, Jiang F, Deng M, et al. 2023 Spatial-temporal changes and driving factors of eco-environmental quality in the Three-North region of China. Journal of Arid Land, 15(3): 231–252.

Lunyolo L D, Khalifa M, Ribbe L. 2021. Assessing the interaction of land cover/land use dynamics, climate extremes and food systems in Uganda. Science of the Total Environment, 753: 142549, doi: 10.1016/j.scitotenv.2020.142549.

Luyssaert S, Jammet M, Stoy P C, et al. 2014. Land management and land-cover change have impacts of similar magnitude on surface temperature. Nature Climate Change, 4: 389–393.

Lyu J, Jiang W, Wang W, et al. 2018. Wetland landscape pattern change and its driving forces in Beijing-Tianjin-Hebei region in recent 30 years. Acta Ecologica Sinica, 38(12): 4492–4503. (in Chinese)

Parihar C M, Yadav M R, Jat S L, et al. 2018. Long-term conservation agriculture and intensified cropping systems: Effects on growth, yield, water, and energy-use efficiency of maize in northwestern India. Pedosphere, 28(6): 952–963.

Powers R P, Jetz W. 2019. Global habitat loss and extinction risk of terrestrial vertebrates under future land-use-change scenarios. Nature Climate Change, 9: 323–329.

Qacami M, Khattabi A, Lahssini S, et al. 2023. Land-cover/land-use change dynamics modeling based on land change modeler. Annals of Regional Science, 70(1): 237–258.

Refati D C, da Silva J L B, Macedo R S, et al. 2023. Influence of drought and anthropogenic pressures on land use and land cover change in the Brazilian semi-arid region. Journal of South American Earth Sciences, 126: 104362, doi: 10.1016/j.jsames.2023.104362.

Shao W Y, Zhang Z P, Guan Q Y, et al. 2024. Comprehensive assessment of land degradation in the arid and semiarid area based on the optimal land degradation index model. Catena, 234: 107563, doi: 10.1016/j.catena.2023.107563.

Silva L, Xavier A, Silva R, et al. 2020. Modeling land cover change based on an artificial neural network for a semiarid river

basin in northeastern Brazil. Global Ecology and Conservation, 21: 00811, doi: 10.1016/j.gecco.2019.e00811.

Song W, Feng Y, Wang Z. 2022. Ecological restoration programs dominate vegetation greening in China. Science of the Total Environment, 848: 157729, doi: 10.1016/j.scitotenv.2022.157729.

Song X P, Hansen M C, Stehman S V, et al. 2018. Global land change from 1982 to 2016. Nature, 560: 639–643.

Song Z F. 2010. Jingtai water supply project: Yingwu reservoir commences construction. Gansu Daily, [2010-10-19(02)]. (in Chinese)

Sy S, Quesada B. 2020. Anthropogenic land cover change impact on climate extremes during the 21st century. Environmental Research Letter, 15(3): 034002, doi: 10.1088/1748-9326/ab702c.

Turner B L, Skole D, Sanderson S, et al. 1995. Land Cover Change Science/Research Plan. Stockholm and Geneva: The International Geosphere Biosphere Program (IGBP) of the International Council for Science (ICSU) and Human Dimensions Programme (HDP) of the International Social Science Council (ISSC).

Turner B L, Lambin E F, Reenberg A. 2007. The emergence of land change science for global environmental change and sustainability. Proceedings of the National Academy of Sciences of the United States of America, 104: 20666–20671.

Wang J F, Xu C D. 2017. Geodetector: Principle and prospective. Acta Geographica Sinica, 72(1): 116–134. (in Chinese)

Wang K, Li X, Lyu X, et al. 2022. Optimizing the land use and land cover pattern to increase its contribution to carbon neutrality. Remote Sensing, 14(19): 3607, doi: 10.3390/su12093607.

Wang X, LESI M, Zhang M. 2019. Ecosystem pattern change and its influencing factors of "Two Barriers and Three Belts". Chinese Journal of Ecology, 38(7): 2138–2148.

Winkler K, Fuchs R, Rounsevell M, et al. 2021. Global land use changes are four times greater than previously estimated. Nature Communications, 12: 2501, doi: 10.1038/s41467-021-22702-2.

Yan J J, Zhang G P, Deng X Y, et al. 2019a. Does climate change or human activity lead to the degradation in the grassland ecosystem in a mountain-basin system in an arid region of China? Sustainability, 11(9): 2618–2632.

Yan X, Li L. 2023. Spatiotemporal characteristics and influencing factors of ecosystem services in Central Asia. Journal of Arid Land, 15(1): 1–19.

Yan X Y, Zhang Q, Yan X M, et al. 2019b. An overview of distribution characteristics and formation mechanisms in global arid areas. Advances in Earth Science, 34(8): 826–841. (in Chinese)

Yang J, Huang X. 2021. The 30 m annual land cover dataset and its dynamics in China from 1990 to 2019. Earth System Science Data, 13(8): 3907–3925.

Yuan X L, Li L H, Chen X, et al. 2015. Effects of precipitation intensity and temperature on NDVI-based grass change over Northern China during the period from 1982 to 2011. Remote Sensing, 7(8): 10164–10183.

Zerouali B, Celso A G S, do Nascimento T V M, et al. 2023. A cloud-integrated GIS for forest cover loss and land use change monitoring using statistical methods and geospatial technology over Northern Algeria. Journal of Environmental Management, 341: 118029, doi: 10.1016/j.jenvman.2023.118029.

Zhang G L, Biradar C M, Xiao X M, et al. 2018. Exacerbated grassland degradation and desertification in Central Asia during 2000–2014. Ecological Applications, 28(2): 442–456.

Zhao Y F, Zhang B, Wang B L, et al. 2012. Spatiotemporal climate change in Hedong Region in Gansu Province in recent 54 years. Arid Zone Research, 29(6): 956–964. (in Chinese)

Appendix

Table S1 Optimal number of intervals and discretization method for driving factors

Land type	1990–1995									1995–2000								
	*X*1	*X*2	*X*3	*X*4	*X*5	*X*6	*X*7	*X*8	*X*9	*X*1	*X*2	*X*3	*X*4	*X*5	*X*6	*X*7	*X*8	*X*9
Cropland	7 QU	7 SD	6 QU	7 SD	7 QU	7 QU	7 SD	7 SD	5 SD	9 QU	8 SD	6 QU	9 SD	8 QU	8 QU	8 GI	9 NB	7 SD
Forest land	6 SD	7 SD	5 QU	6 QU	6 QU	7 QU	7 GI	6 QU	7 GI	9 QU	3 EI	8 QU	9 QU	9 QU	9 QU	9 QU	7 QU	8 QU
Grassland	9 QU	9 SD	9 QU	8 QU	9 QU	8 QU	9 SD	7 GI	9 NB	8 QU	8 SD	6 QU	8 SD	8 QU	8 QU	8 GI	8 SD	7 SD
Water body	4 GI	9 QU	8 QU	8 QU	9 QU	6 QU	5 QU	9 NB	9 QU	9 QU	8 SD	9 QU	7 QU	8 QU	9 QU	9 QU	8 EI	7 SD
Bare land	6 SD	7 SD	7 QU	5 GI	7 QU	7 QU	7 GI	7 NB	5 GI	7 QU	7 QU	7 QU	7 QU	6 SD	6 QU	7 GI	6 SD	6 QU
Construction land	5 QU	7 SD	3 GI	7 QU	5 QU	7 QU	6 QU	7 SD	7 NB	7 QU	9 QU	5 SD	3 GI	8 NB	7 QU	9 SD	6 GI	9 QU

Land type	2000–2005									2005–2010								
	*X*1	*X*2	*X*3	*X*4	*X*5	*X*6	*X*7	*X*8	*X*9	*X*1	*X*2	*X*3	*X*4	*X*5	*X*6	*X*7	*X*8	*X*9
Cropland	8 QU	9 QU	8 QU	9 SD	6 QU	5 QU	7 GI	9 QU	9 QU	7 QU	7 SD	7 QU	7 EI	9 QU	7 QU	5 GI	8 QU	7 SD
Forestland	8 QU	9 QU	7 GI	6 SD	8 QU	3 GI	9 GI	5 GI	9 SD	9 QU	7 SD	9 QU	9 QU	8 QU	9 QU	8 QU	5 GI	9 QU
Grassland	5 QU	7 QU	7 GI	4 GI	6 QU	5 QU	7 GI	5 GI	7 QU	6 QU	7 SD	7 QU	9 SD	9 QU	9 QU	3 GI	8 QU	7 SD
Water body	8 QU	7 QU	6 GI	8 QU	7 QU	9 QU	5 QU	5 GI	9 SD	9 QU	7 SD	7 QU	7 QU	9 QU	9 QU	3 GI	9 QU	8 EI
Bare land	9 QU	4 GI	9 QU	9 QU	9 QU	9 QU	9 GI	9 EI	9 QU	9 QU	9 QU	9 QU	7 GI	9 QU	9 QU	9 QU	8 QU	9 QU
Construction land	8 QU	7 SD	5 SD	9 SD	7 QU	5 QU	9 QU	6 EI	9 SD	9 QU	8 SD	9 QU	9 GI	7 GI	5 SD	8 NB	8 QU	8 QU

Land type	2010–2015									2015–2020								
	*X*1	*X*2	*X*3	*X*4	*X*5	*X*6	*X*7	*X*8	*X*9	*X*1	*X*2	*X*3	*X*4	*X*5	*X*6	*X*7	*X*8	*X*9
Cropland	9 QU	6 EI	9 QU	9 GI	9 QU	8 QU	6 NB	9 QU	8 QU	6 NB	9 QU	6 QU	8 QU	8 QU	6 NB	7 QU	8 SD	8 QU
Forest land	9 QU	9 QU	9 QU	8 QU	8 QU	9 QU	9 QU	8 GI	8 EI	9 QU	7 QU	9 QU	9 QU	9 QU	9 QU	7 QU	9 QU	7 EI
Grassland	9 QU	6 EI	9 QU	5 QU	9 QU	8 QU	6 NB	9 QU	8 QU	6 NB	8 QU	9 QU	7 QU	5 QU	6 NB	7 QU	9 QU	8 SD
Water body	8 QU	6 EI	3 SD	9 QU	9 QU	9 QU	9 QU	8 SD	8 GI	9 QU	8 SD	9 QU	9 QU	9 QU	8 QU	9 QU	9 QU	9 QU
Bare land	9 QU	6 QU	9 QU	9 QU	7 GI	9 QU	6 NB	9 QU	9 SD	7 QU	8 SD	9 QU	9 QU	7 QU	9 QU	6 SD	8 GI	9 SD
Construction land	9 QU	7 QU	4 GI	7 GI	7 GI	3 SD	9 QU	9 EI	8 QU	8 QU	8 QU	7 QU	8 QU	8 QU	9 QU	9 QU	9 QU	6 EI

Land type	1990–2020								
	*X*1	*X*2	*X*3	*X*4	*X*5	*X*6	*X*7	*X*8	*X*9
Cropland	7 SD	7 SD	9 QU	6 QU	8 QU	8 QU	4 GI	8 GI	8 QU
Forest land	7 SD	7 SD	8 QU	6 SD	8 QU	8 QU	9 QU	9 SD	9 QU
Grassland	7 SD	7 SD	7 QU	4 EI	9 QU	8 QU	4 GI	8 GI	9 QU
Water body	9 QU	3 GI	4 GI	9 QU	9 QU	9 QU	8 QU	9 EI	8 SD
Bare land	9 QU	9 QU	6 QU	9 QU	9 QU	8 QU	9 QU	9 QU	9 QU
Construction land	9 QU	8 QU	9 QU	8 QU	8 QU	6 QU	8 QU	9 EI	9 QU

Note: *X*1–*X*9 means nine explanatory variables that are listed in Table 1. Initial number of intervals are set as 3–8. QU, quantile method; GI, geometrical interval; SD, standard deviation; NB, natural breaks method; EI, equal-interval method.